Taylor & Francis
Taylor & Francis Group

Electric Power Components and Systems

ISSN: 1532-5008 (Print) 1532-5016 (Online) Journal homepage: www.tandfonline.com/journals/uemp20

An Effective Four-Level Voltage Switching State Algorithm for Direct Torque Controlled Open End Winding Induction Motor Drive by Using Two Two-Level Inverters

Kunisetti V Praveen Kumar & Thippiripati Vinay Kumar

To cite this article: Kunisetti V Praveen Kumar & Thippiripati Vinay Kumar (2017) An Effective Four-Level Voltage Switching State Algorithm for Direct Torque Controlled Open End Winding Induction Motor Drive by Using Two Two-Level Inverters, Electric Power Components and Systems, 45:19, 2175-2187, DOI: 10.1080/15325008.2017.1405104

To link to this article: https://doi.org/10.1080/15325008.2017.1405104

Published online: 13 Feb 2018.

Electric Power Components and Systems, 45(19):2175–2187, 2017

ISSN: 1532-5008 print / 1532-5016 online
DOI: 10.1080/15325008.2017.1405104

An Effective Four-Level Voltage Switching State Algorithm for Direct Torque Controlled Open End Winding Induction Motor Drive by Using Two Two-Level Inverters

Kunisetti V Praveen Kumar and Thippiripati Vinay Kumar
Electrical Engineering Department, National Institute of Technology, Warangal, Telangana, India

CONTENTS

Abstract—This paper introduces an effective four-level voltage switching state algorithm for direct torque controlled open end winding induction motor drive with two-two level inverters in dual mode. In the recent days, direct torque control of open end winding induction motor drive became an interesting area for researchers because it provides high dynamic performance and instantaneous control of stator flux and torque. It is more important especially in applications like propulsion and hybrid electric vehicles they require ripple free torque. The direct torque control provides high flux, torque ripple, and variable switching frequency. This paper introduces an effective voltage switching state algorithm for an open end winding induction motor drive to reduce torque and flux ripple at different frequencies of operation. The experimental results show that the proposed algorithm reduces torque and flux ripples without losing features of conventional direct torque control (DTC) algorithm and in addition it provides multi-level operation.

Keywords: direct torque control, open end winding induction motor, voltage switching states, speed control, multi-level inversion and torque ripple
Received 16 June 2016; accepted 22 October 2017
Address correspondence to Kunisetti V Praveen Kumar, Electrical Engineering Department, National Institute of Technology, Warangal, Telangana 506004, India. E-mail: kvpraveenkumar15@gmail.com; Thippiripati Vinay Kumar, Electrical Engineering Department, National Institute of Technology, Warangal, Telangana 506004, India. E-mail: tvinay.nitw@gmail.com
Color versions of one or more of the figures in the article can be found online at www.tandfonline.com/uemp.

1. INTRODUCTION

Induction motor drives are very popular for industrial applications due to its robust construction and maintenance-free operation. In some applications, like marine and propulsion still DC motors are used due to its speed control capability. The DC motors have wide limitations: low torque to inertia ratio and requirement of regular maintenance [1]. The induction motors can provide high dynamic performance and wide range of speed control like DC motor. Fast dynamic response is obtained by using direct torque control technique. The scheme of direct torque control eliminates drawbacks of popular vector control technique (field-oriented control) of induction motor and it was introduced by Takahashi and Noguchi [2]. The direct torque control has high dynamic performance and it has simple algorithm to control torque and flux by choosing appropriate inverter switching states. The selected inverter switching states should restrict the torque and flux

errors within the hysteresis bands [3]. During the last three decades, vast research has been carried on direct torque control of induction motors. The scheme of DTC produces high torque, flux ripples and it uses hysteresis controllers, these produce variable switching frequency and lead to high sampling time [4]. To overcome the limitations of DTC constant switching frequency technique was implemented by Idris and Yatim [5]. It requires two triangular wave form generators, two comparators, and a PI controller in addition to DTC algorithm.

Kang-Sul introduced implementation of DTC scheme by using space vector modulation to obtain constant switching frequency [6]. The DTC-SVM gives constant switching frequency, but it requires reference stator voltage space vector [7]–[9]. Reference stator voltage space vector calculation is very difficult and it is synthesized within sampling frequency. Noguchi et al. implemented dithering technique to enlarge switching frequency in DTC-SVM [10], but it needs a high-frequency triangular wave form and proper PI controller. Ambrožic implemented a novel technique to overcome torque ripple. The voltage vectors are applied by inverter to reach torque controller to its upper or lower bands for certain time intervals and the application of voltage vectors is independent of sampling time. This is implemented only for two-level inverter fed induction motor drive [11]. In [12], direct load angle control method is implemented based on incremental change of load angle with constant switching frequency. In this method, induction motor was implemented in synchronous reference frames rather than regular stationary reference frames to estimate incremental change of load angle. In [13], a novel direct torque control algorithm is implemented, in this required amount of reference stator flux is obtained by utilizing sum of change in load angle, load angle and rotor flux angle. This method is simpler and requires less computational efforts. It needs load angle estimator in addition to DTC. In order to maintain lesser torque and flux ripple, multi-level inverter-based direct torque control scheme is implemented [14].

In [15], a novel switching algorithm is implemented for induction motor fed with pulse width modulated current source inverter. The switching algorithm is based on stator flux reference. This method developed on space vector modulation so it needs reference stator current component. In [16], a comparative study of DTC-SVM with controllers and DTC-SVM with sliding mode controllers was developed and it focuses on maintaining constant switching frequency and torque ripple reduction through an adaptive model.

In [17], comparison of various types of model predictive schemes for medium voltage induction motors was studied through simulation. This paper focuses on longer horizons and performance of motor at different operating points was studied. In this paper, only simulation studies are exhibited. Model predictive control requires high-speed processor for longer prediction horizons and it requires more number of instruction cycles when compared with DTC of induction motor.

From the literature, it is observed that the torque and flux ripples can be reduced by using different methods. The torque and flux ripples can be easily reduced by using multi-level inverter configuration [14]. To reduce ripples in motor drive, this paper is developed with four-level inverter for open end winding induction motor. The multi-level inverter fed induction motor drive is obtained by using open end winding configuration [18]. Open end winding configuration of induction motor was obtained by opening the stator terminals of induction motor by feeding with two two-level inverters on both sides of stator winding [19], [20]. By implementing open end winding induction motor, it is easy to obtain multi-level inversion, instead of going for different types of multi-level inverters. In [21], a four-level inverter drive is obtained by using DC link voltages in the ratio of 2:1 with nested rectifier on one side of stator winding. This eliminates zero-sequence current component by restoring decoupled space vector pulse width modulation. Arbind and Fernandez implemented direct torque control of open end winding induction motor by using three-level inverter scheme based on space vector modulation for marine and ship propulsion applications. In [14], a new and effective switching state algorithm is developed for induction motor to operate at different speeds. In this method, it requires three individual DC voltage sources and it uses 18 switches for its operation. Therefore, it is felt that instead of using higher number of switches for four-level configuration there is a scope to reduce number of switches. Hence, the proposed four-level inverter is implemented with the help of only 12 switches for induction motor drive with open end windings.

The objectives of proposed DTC algorithm is to: implement an effective voltage switching state algorithm for an open end winding induction motor (OEWIM) to reduce torque and flux ripple with the help of four-level inversion based on two two-level inverters, location of voltage space vectors, application of voltage space vectors based on operating frequencies, utilizing necessary mathematical models, algorithm for reduction of torque and flux ripple, and hardware implementation of proposed scheme to observe its behavior. The proposed algorithm is implemented with four-level configuration so it has less dv/dt stress. The open end winding configuration is developed with two independent DC sources and the effects of common mode voltages are reduced. In this paper, experimental verification was performed for DTC of open end winding induction motor drive with two-level inverter configuration and four-level configuration. The

two-level configuration was obtained by operating the inverters with DC link voltage of 1:1 ratio whereas four-level configuration was obtained by operating the inverters with 2:1 ratio. Finally, it is noticed that the proposed algorithm reduces torque and flux ripples at all frequencies of operation of motor drive without losing the features of conventional DTC.

2. CONTROL METHOD

2.1. Proposed Four-Level Direct Torque Control

The power circuit diagram and the block diagram of proposed four-level DTC strategy are shown in Figure 1(a) and 1(b), respectively. The four-level inversion scheme is obtained by energizing the open-end winding induction motor with two two-level inverters on both sides with asymmetrical configuration. The asymmetrical configuration was obtained by feeding the two inverters with voltages $2V_{dc}/3$ and $V_{dc}/3$.

In the block diagram of proposed DTC strategy, ω_{ref} indicates reference speed, ω_e represents actual speed of induction motor, T_{ref}^* indicates reference torque developed from speed PI controller, T_e indicates actual electromagnetic torque of motor, ψ_{ref} indicates reference stator flux, ψ_s indicates actual flux of induction motor, (S_a, S_b and S_c) are the gating signals applied to voltage source inverter-1, and (S'_a, S'_b and S'_c) are the gating signals applied to voltage source inverter-2.

In Figure 1(a), two voltage source inverters are energized with DC link voltage ratio of 2:1. Therefore, it gives 64 voltage space vectors. Out of 64 voltage space vectors, it gives 36 active voltage space vectors because the four-level inverter provides high redundancy of switching states.

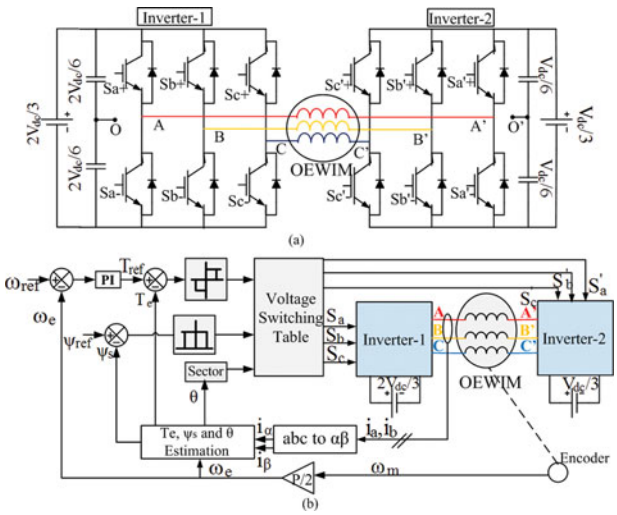

FIGURE 1. (a) Power circuit diagram. (b) Block diagram of proposed DTC.

Inverter 1			Inverter 2			Voltage space vector
Sa	Sb	Sc	Sa'	Sb'	Sc'	
0	0	0	0	0	0	V_0
1	0	0	1	0	0	V_1
1	1	0	1	1	0	V_2
0	1	0	0	1	0	V_3
0	1	1	0	1	1	V_4
0	0	1	0	0	1	V_5
1	0	1	1	0	1	V_6
1	0	0	1	1	1	V_7
1	0	0	1	0	1	V_8
1	1	0	1	1	1	V_9
0	1	0	0	1	1	V_{10}
0	1	0	1	1	1	V_{11}
0	1	0	1	1	0	V_{12}
0	1	1	1	1	1	V_{13}
0	0	1	1	0	1	V_{14}
0	0	1	1	1	1	V_{15}
0	0	1	0	1	1	V_{16}
1	0	1	1	1	1	V_{17}
1	0	0	1	1	0	V_{18}
1	0	0	0	1	1	V_{19}
1	0	0	0	0	1	V_{20}
1	1	0	0	1	1	V_{21}
1	1	0	0	0	1	V_{22}
1	1	0	1	0	1	V_{23}
0	1	0	0	0	1	V_{24}
0	1	0	1	0	1	V_{25}
0	1	0	1	0	0	V_{26}
0	1	1	1	0	1	V_{27}
0	1	1	1	0	0	V_{28}
0	1	1	1	1	0	V_{29}
0	0	1	1	0	0	V_{30}
0	0	1	1	1	0	V_{31}
0	0	1	0	1	0	V_{32}
1	0	1	1	1	0	V_{33}
1	0	1	0	1	0	V_{34}
1	0	1	0	1	1	V_{35}
1	0	0	0	1	0	V_{36}

TABLE 1. Switching states of inverters 1 and 2.

Table 1 indicates the switching states of individual switches used in inverter. The switches are turned to realize respective switching states of two inverters. The switching states of inverter for two-level configuration are calculated by using following equations:

$$V_{01} = \frac{2}{3} * \frac{2V_{dc}}{3} * \left(S_a + S_b e^{j\frac{2\pi}{3}} + S_c e^{j\frac{4\pi}{3}}\right) \quad (1)$$

and

$$V_{02} = \frac{2}{3} * \frac{V_{dc}}{3} * \left(S'_a + S'_b e^{j\frac{2\pi}{3}} + S'_c e^{j\frac{4\pi}{3}}\right). \quad (2)$$

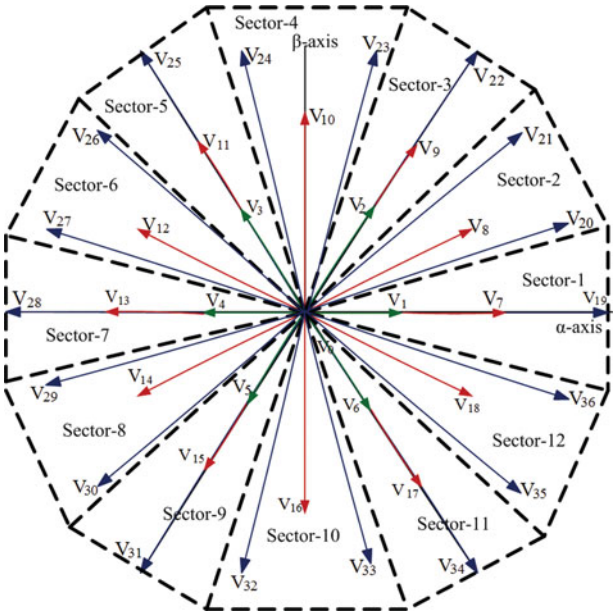

FIGURE 2. Classification of voltage vectors based on different operating frequencies.

The space vector locations of proposed four-level inverter are as shown in Figure 2. To obtain four-level configuration, the two inverters are operated with unequal DC link voltages and they are operated in duality mode. Therefore, from the mathematical calculations, four-level inverter produces 36 active voltage space vectors and these are represented in Figure 2 and as shown in Table 1. The active voltage space vectors of the four-level inverter are obtained from all combinations of switching states of inverter and the open end winding configuration offers high redundancy of switching states. Here an example is illustrated, how to find out voltage space vector. Let us take voltage space vector V_1. It is obtained by operating inverter-1 with switching states of (1,0,0) and inverter-2 with switching states of (1,0,0). Then by using Eqs. (1) and (2), the voltage space vector V_1 can be written as

$$V_s = (V_{01} - V_{02})\,. \tag{3}$$

The resultant voltage space vector for all the switching states of inverter is obtained by using (3). On simplifying (3) with switching states of (1,0,0) and (1,0,0), the resultant voltage vector is obtained, its magnitude is $V_{dc}/3$ and phase angle is zero, hence it is named as V_1. In similar, on applying switching states (1,0,0) and (1,1,1), voltage space vector V_7 is obtained. By applying the switching states of (1,0,0) and (0,1,1), voltage space vector V_{19} is obtained.

On applying all possible switching states to inverter, it gives 36 active voltage space vectors. These space vectors are arranged in Figure 2. The voltage space vectors are divided into three groups for different frequencies of operation. The voltage space vectors V_{19} to V_{36} are applied for higher frequencies of operation. The voltage space vectors V_7 to V_{18} are applied for medium frequencies. The voltage space vectors V_1 to V_6 are applied for low frequencies of operation. These 36 active space vectors are divided into three groups to maintain constant *V*/*f* ratio. Based on rotor speed, the active voltage space vector is divided into three categories. These are low, medium and high frequency space vectors. From Figure 2, the active voltage space vector is divided into 18 sectors for high frequencies of operation and 12 sectors for medium and low frequencies of operation. For high frequencies of operation, each sector is divided into 20°. The division of sectors is explained as below. Sector-1 of active voltage space vector is from 350° to 10°. Sector-2 of active voltage space vector is from 10° to 30°. Sector-3 of active voltage space vector is from 30° to 50°. Sector-4 of active voltage space vector is from 50° to 70°. Sector-5 of active voltage space vector is from 70° to 90°. Sector-6 of active voltage space vector is from 90° to 110°. Sector-7 of active voltage space vector is from 110° to 130°. Sector-8 of active voltage space vector is from 130° to 150°. Sector-9 of active voltage space vector is from 150° to 170°. Sector-10 of active voltage space vector is from 170° to 190°. Sector-11 of active voltage space vector is from 190° to 210°. Sector-12 of active voltage space vector is from 210° to 230°. Sector-13 of active voltage space vector is from 230° to 250°. Sector-14 of active voltage space vector is from 250° to 270°. Sector-15 of active voltage space vector is from 270° to 290°. Sector-16 of active voltage space vector is from 290° to 310°. Sector-17 of active voltage space vector is from 310° to 330°. Sector-18 of active voltage space vector is from 330° to 350°.

For medium and low frequencies of operation, each sector is divided into 30°. The division of sectors is explained as below. Sector-1 of active voltage space vector is from 345° to 15°. Sector-2 of active voltage space vector is from 15° to 45°. Sector-3 of active voltage space vector is from 45° to 75°. Sector-4 of active voltage space vector is from 75° to 105°. Sector-5 of active voltage space vector is from 105° to 135°. Sector-6 of active voltage space vector is from 135° to 165°. Sector-7 of active voltage space vector is from 165° to 195°. Sector-8 of active voltage space vector is from 195° to 225°. Sector-9 of active voltage space vector is from 225° to 255°. Sector-10 of active voltage space vector is from 255° to 285°. Sector-11 of active voltage space vector is from 285° to 315°. Sector-12 of active voltage space vector is from 315° to 345°. The proposed algorithm is developed based on flux space vector is assumed to be lie in sector-1.

Flux error	Torque error	Sector 1	2	3	4	5	6	7	8	9	10	11	12	13	14	15	16	17	18
1	1	V_{22}	V_{23}	V_{24}	V_{25}	V_{26}	V_{27}	V_{28}	V_{29}	V_{30}	V_{31}	V_{32}	V_{33}	V_{34}	V_{35}	V_{36}	V_{19}	V_{20}	V_{21}
	−1	V_{34}	V_{35}	V_{36}	V_{19}	V_{20}	V_{21}	V_{22}	V_{23}	V_{24}	V_{25}	V_{26}	V_{27}	V_{28}	V_{29}	V_{30}	V_{31}	V_{32}	V_{33}
−1	1	V_{25}	V_{26}	V_{27}	V_{28}	V_{29}	V_{30}	V_{31}	V_{32}	V_{33}	V_{34}	V_{35}	V_{36}	V_{19}	V_{20}	V_{21}	V_{22}	V_{23}	V_{24}
	−1	V_{31}	V_{32}	V_{33}	V_{34}	V_{35}	V_{36}	V_{19}	V_{20}	V_{21}	V_{22}	V_{23}	V_{24}	V_{25}	V_{26}	V_{27}	V_{28}	V_{29}	V_{30}

TABLE 2. Selection of active voltage vector for high-frequency operation.

2.2. High Frequency of Operation (Above 70% of Rated Frequency to Rated Frequency)

During high frequency of operation of open end induction motor drive, to control stator flux and torque the voltage space vectors V_{19} to V_{36} and a null vector V_0 are utilized to realize resultant space vector. In Figure 2, if the resultant stator flux vector ψ_s is in sector-1, then by applying voltage space vectors V_{20}, V_{21}, V_{22}, and V_{36} its magnitude increases, whereas by applying V_{24}, V_{25}, V_{31}, and V_{32} its magnitude decreases. In the same sector to reduce positive torque error, V_{21}, V_{22}, and V_{23} are utilized, whereas for the reduction of negative torque error V_{34}, V_{35}, and V_{36} are used. In high-speed operation to maintain constant *V/f* ratio, the voltage vectors V_1 to V_{18} should not be applied. The selection of voltage vectors for high frequencies is shown in Table 2.

2.3. Medium Frequency of Operation (In Between 30 to 70% of Rated Speed)

In the medium-frequency range, to control stator flux and torque of open end winding induction motor drive, the voltage space vectors V_7 to V_{18} and a null vector V_0 are used to realize the resultant space vector. In Figure 2, if the resultant stator flux vector $\psi_s$is in sector-1, then by applying voltage space vectors V_8, V_9, V_{17}, and V_{18} its magnitude increases, whereas by applying V_{11}, V_{12}, V_{14}, and V_{15} its magnitude decreases. In the same sector to reduce positive torque error, V_8, V_9, and V_{10} are utilized, whereas for the reduction of negative torque error V_{16}, V_{17}, and V_{18} are used. In medium speed operation to maintain constant *V/f* ratio, the voltage vectors V_1 to V_6 and V_{18} to V_{36} should not be applied. The selection of active voltage vectors for medium frequencies of operation is shown in Table 3.

2.4. Low Frequency of Operation (Less than 30% of Rated Speed)

In the low-frequency range, to control stator flux and torque of open end winding induction motor drive, the voltage space vectors V_1 to V_6 and a null vector V_0 are used to realize the resultant space vector. In Figure 2, if the resultant flux vector ψ_s is in sector-1, then by applying voltage space vectors V_2 and V_6 its magnitude increases, whereas by applying V_5 and V_3 its magnitude decreases. In the same sector to reduce positive torque error V_2 and V_3 are utilized, whereas for the reduction of negative torque error V_5 and V_6 are used. In low-speed operation to maintain constant *V/f* ratio, the voltage vectors V_{18} to V_{36} should not be applied. The selection of active voltage vectors for low frequencies of operation is shown in Table 4.

2.5. Algorithm to Reduce Torque and Flux Ripple

From [23], the torque equation of induction motor in stationary reference frames is given by

$$T_e = \frac{3}{2} * \frac{P}{2} \left(\overline{\psi_s} \otimes \overline{i_s} \right) \tag{4}$$

Simplification of (4) gives

$$T_e = \frac{3}{2} * \frac{P}{2} \left(\psi_{\alpha s} i_{\beta s} - \psi_{\beta s} i_{\alpha s} \right). \tag{5}$$

From (5), to obtain less torque ripple it is required to maintain low current and flux ripples. By controlling flux of the

Flux error	Torque error	Sector 1	2	3	4	5	6	7	8	9	10	11	12
1	1	V_9	V_{10}	V_{11}	V_{12}	V_{13}	V_{14}	V_{15}	V_{16}	V_{17}	V_{18}	V_7	V_8
	−1	V_{17}	V_{18}	V_7	V_8	V_9	V_{10}	V_{11}	V_{12}	V_{13}	V_{14}	V_{15}	V_{16}
−1	1	V_{11}	V_{12}	V_{13}	V_{14}	V_{15}	V_{16}	V_{17}	V_{18}	V_7	V_8	V_9	V_{10}
	−1	V_{15}	V_{16}	V_{17}	V_{18}	V_7	V_8	V_9	V_{10}	V_{11}	V_{12}	V_{13}	V_{14}

TABLE 3. Selection of active voltage vector for medium-frequency operation.

Flux error	Torque error	Sector											
		1	2	3	4	5	6	7	8	9	10	11	12
1	1	V_2	V_2	V_3	V_3	V_4	V_4	V_5	V_5	V_6	V_6	V_1	V_1
	−1	V_6	V_6	V_1	V_1	V_2	V_2	V_3	V_3	V_4	V_4	V_5	V_5
−1	1	V_3	V_3	V_4	V_4	V_5	V_5	V_6	V_6	V_1	V_1	V_2	V_2
	−1	V_5	V_5	V_6	V_6	V_1	V_1	V_2	V_2	V_3	V_3	V_4	V_4

TABLE 4. Selection of active voltage vector for low-frequency operation.

induction motor, torque can be controlled. Therefore, torque and flux ripples are dependent on voltage. If the voltage ripple is decreased, then it reduces flux ripple. The stator voltage equation of open end winding induction motor (output voltage of inverter) is given by

$$v(t) = R_s i_s + L_s \frac{di_s}{dt} + e, \tag{6}$$

where $v(t)$ is the inverter output voltage, R_s is the stator resistance, L_s is the stator inductance, i_s is the stator current, and e is the developed voltage of motor. The inverter output voltage $v(t)$ has 36 locations for four-level inverter depending on its all possible switching states. Equation (6) can be rewritten as

$$\frac{di_s}{dt} = \left(\frac{v(t) - e - R_s i_s}{L_s} \right). \tag{7}$$

On neglecting stator voltage drop ($R_s i_s$) of induction motor, the rate of change of stator current (di_s/dt) is dependent on inverter output voltage and developed voltage of motor. To obtain low current ripple, the rate of change of stator current should be less. It is maintained by selecting proper switching vectors. The rate of change of stator current (di_s/dt) plays an important role to reduce torque ripple in steady state and it is illustrated by (7). On simplification of (4) and from [14, 22], the expressions of torque and rotor flux can be written as

$$T_e = \frac{3}{2} * \frac{P}{2} * \frac{L_m}{kL_r} \left(\overline{\psi_r} \otimes \overline{\psi_s} \right) \tag{8}$$

$$\psi_r = \frac{L_r}{L_m} \psi_s - \sigma i_s. \tag{9}$$

where ψ_s is the stator flux, ψ_r is the rotor flux, L_m is the mutual inductance, and L_r is the rotor inductance.

And

$$\sigma = \frac{L_s L_r - L_m^2}{L_m}; k = \frac{L_s L_r - L_m^2}{L_r}.$$

Performing differentiation for (9) with respect to time, it can be written as

$$\frac{d\psi_r}{dt} = \frac{L_r}{L_m} * \frac{d\psi_s}{dt} - \sigma \frac{di_s}{dt} \tag{10}$$

and

$$\frac{di_s}{dt} = (k_1 V_s - j k_2 \psi_r \omega_r). \tag{11}$$

Here

$$k_1 = \frac{L_r}{\sigma L_m}; k_2 = \frac{1}{\sigma}.$$

From (10) and (11), rate of change of stator current depends on voltage applied to stator and speed of rotor flux. di_s/dt is independent of rotor flux so it is maintained as constant by applying suitable voltage vector. If rotor flux is kept constant, then torque of induction motor is dependent only on stator flux and current. By maintaining lower current ripple, the ripples in flux and torque can be reduced significantly.

In the expression of di_s/dt, the first component indicates stator voltage vector and second component gives magnitude of back EMF. The back EMF depends on rotor flux speed ($jk_2\psi_r\omega_r$) only and rotor flux is kept constant. The deviation of current ripple with respect to variation of operating frequencies is as shown in Figure 3.

For high-speed operations, if the flux vector is assumed to be in sector-1 then by applying V_{22} torque and flux can be increased. By applying V_{23} it will result in rapid change of load angle so torque can increase but flux will decrease rapidly. Hence, for high-speed operation if stator flux is in sector-1 then voltage vector should be applied. To decrease torque and flux, V_{31} has to be applied.

For medium speeds of operation, if flux space vector is in sector-1 then the suitable voltage vector applied to increase flux and torque is V_9. For medium frequencies, V_{22} should not be used, if we apply V_{22} for medium frequencies operation then V/f ratio should not be maintained as constant. By applying V_9 voltage vector, the magnitude of voltage applied is when compared with V_{22} and also it decreases variations in rate of change of stator current di_s/dt.

For low speeds of operation, if the flux space vector is in sector-1 then the suitable voltage vector applied to increase torque and flux is V_2. The voltage vector V_2 for low speeds of operation maintains: constant V/f ratio, reduced current ripple, constant rotor flux, and less flux and torque ripple.

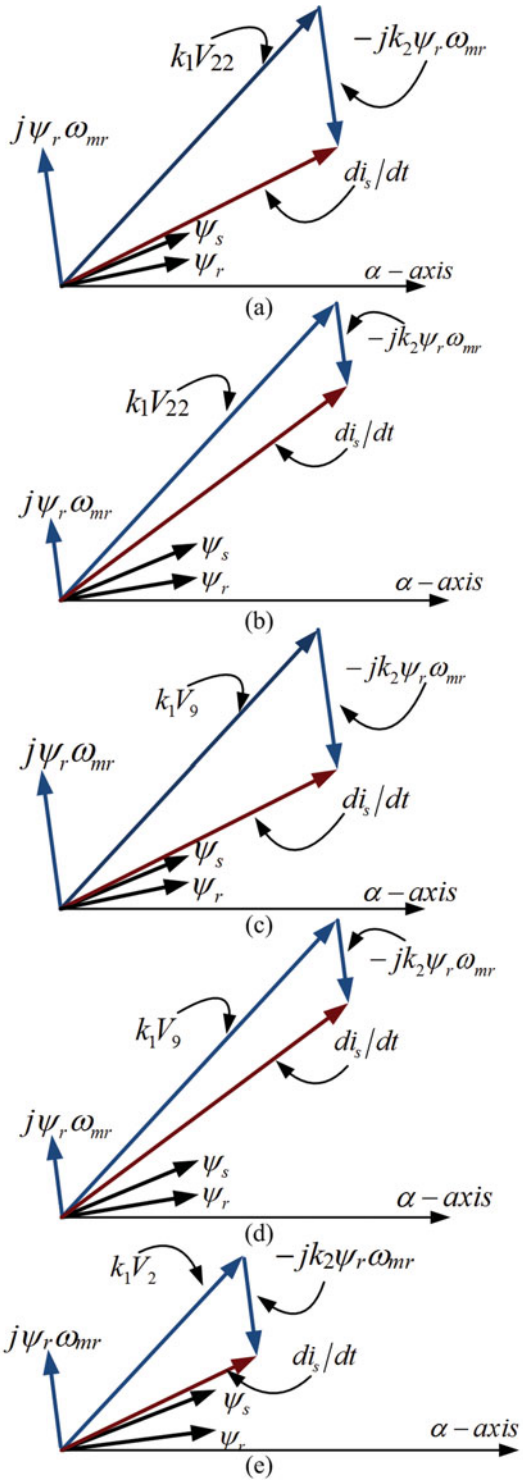

FIGURE 3. Incremental change in stator current to increase torque and flux: (a) High frequency of operation, (b) medium frequency of operation, (c) medium frequency of operation, (d) low frequency of operation, and (e) low frequency of operation.

Figure 3 illustrates variation of current ripple with respect to high, medium, and low speed of operation and application of suitable voltage vectors for flux space vector in sector-1. Tables 2–4 show the application of suitable voltage vectors with respect to rotor speed to maintain lesser ripple in flux and torque.

3. EXPERIMENTAL RESULTS

From the mathematical analysis of inverter and control circuit, the proposed algorithm is implemented with dspace-1104 system by interfacing it with MATLAB/simulink. Dspace-1104 is used to deliver gating signals for inverters. An experiment is conducted on the developed hardware to verify the proposed algorithm.

The experiment was conducted on open end winding induction motor drive to operate at different speeds of operation. For convenience, the results are shown for three different speeds of operation. For high speeds of operation, the motor drive is set to operate at 250 rad/sec, for medium speeds of operation it is set to operate at 160 rad/sec, and for low speeds of operation it is set to operate at 80 rad/sec. The rated speed of motor drive is 1440 RPM, so it is approximately 300 rad/sec (frequency in electrical rad/sec). The behavior of motor drive during forward and reverse motoring conditions is also exhibited.

Figures 4–11 represent experimental waveforms of proposed and DTC of induction motor using four-level and two-level inverter configuration. Figures 4 and 5 represent actual speed versus reference speed of motor drive for two-level and proposed DTC, respectively. Figures 4(a) and 5(a) indicate forward motoring of drive at 80 rad/sec, 160 rad/sec, and 250 rad/sec for two-level DTC and proposed DTC. Figures 4(b) and 5(b) represent forward motoring of drive at 250 rad/sec, 160 rad/sec, and 80 rad/sec for two-level and proposed DTC. Figures 4(c) and 5(c) indicate speed reversal of motor drive from −80 rad/sec to 80 rad/sec for two-level and proposed DTC. From experimental results, proposed DTC provides less variation from actual speed to reference speed.

Figures 6 and 7 represent actual speed and flux of motor drive in forward and reverse motoring conditions. The reference stator flux to motor drive is set at 0.8 Wb. Hence, the proposed and two-level DTC operates at 0.8 Wb.

Figures 6(a) and 7(a) indicate actual speed and flux of motor drive in forward motoring and motor drive is set to operate at 0.8 Wb with variation of speeds 80 rad/sec, 160 rad/sec, and 250 rad/sec for two-level and proposed DTC. Figures 6(b) and 7(b) indicate actual speed and flux of motor drive in

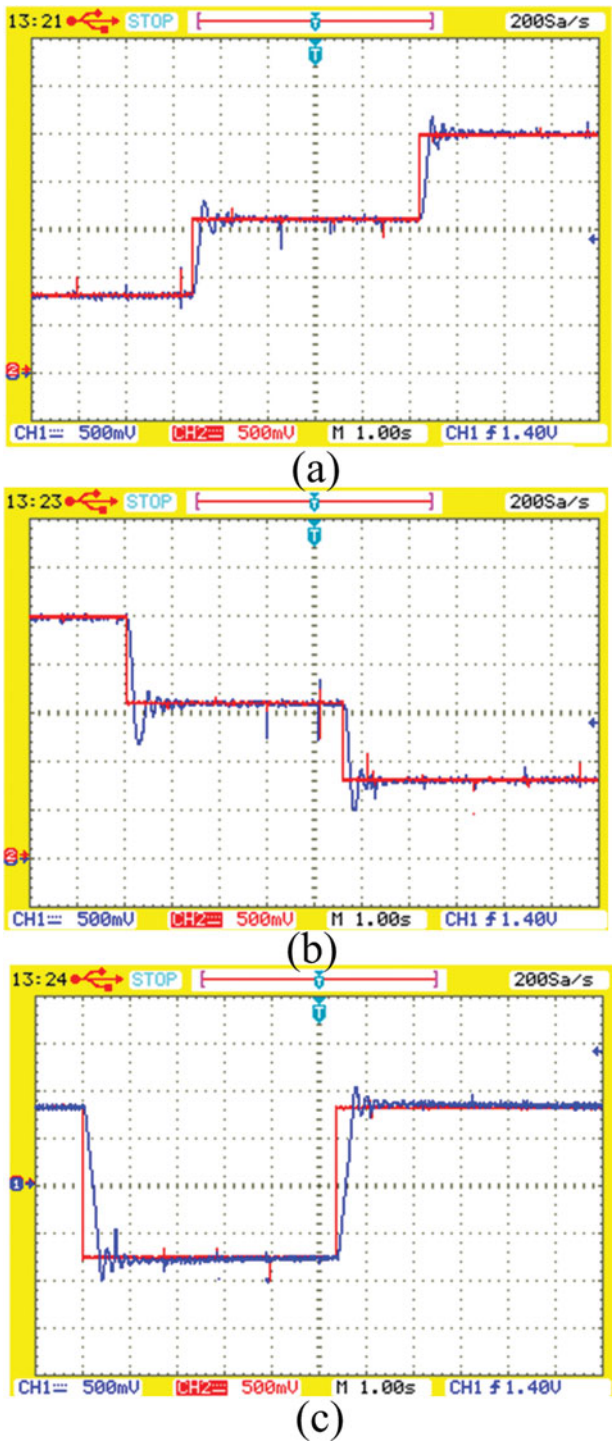

FIGURE 4. Experimental response of two-level DTC: (a) Forward motoring (speed increase). (b) Forward motoring (speed decrease). (c) Variation of speed from reverse motoring to forward motoring. (Red: Reference speed and 1 Div = 50 rad/sec) (Blue: Actual speed and 1 Div = 50 rad/sec).

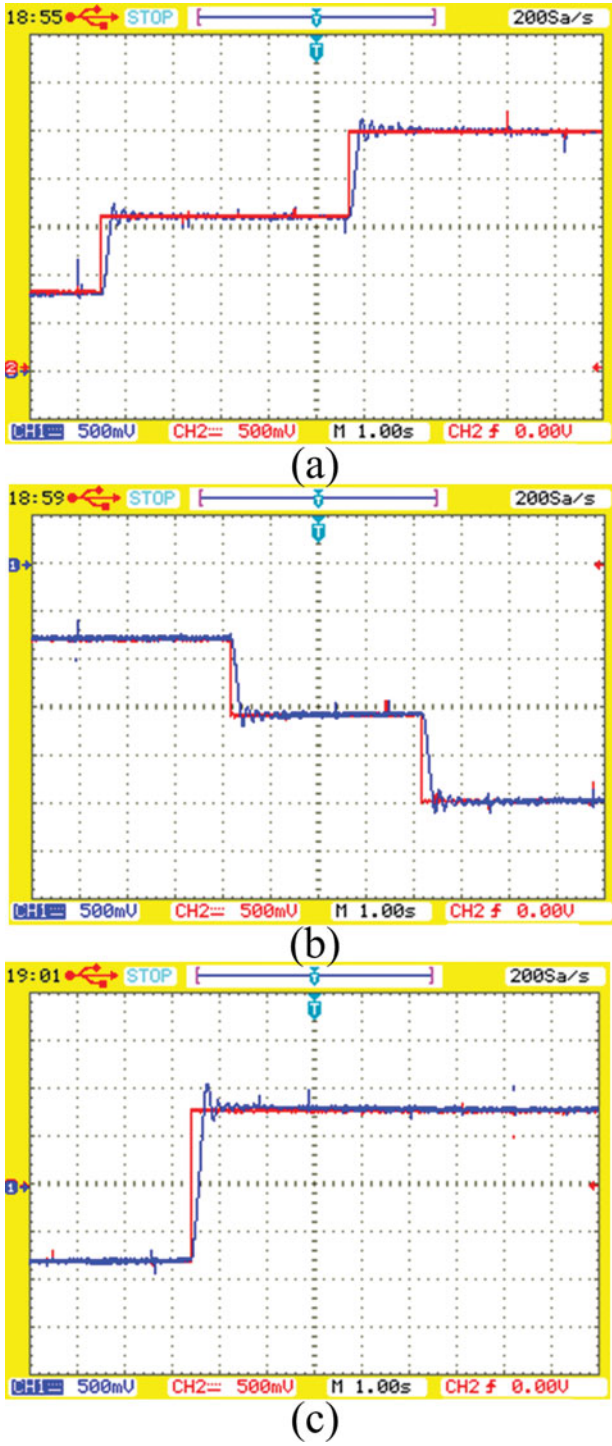

FIGURE 5. Experimental response of proposed DTC: (a) Forward motoring (speed increase). (b) Forward motoring (speed decrease). (c) Variation of speed from reverse motoring to forward motoring. (Red: Reference speed and 1 Div = 50 rad/sec) (Blue: Actual speed and 1 Div = 50 rad/sec).

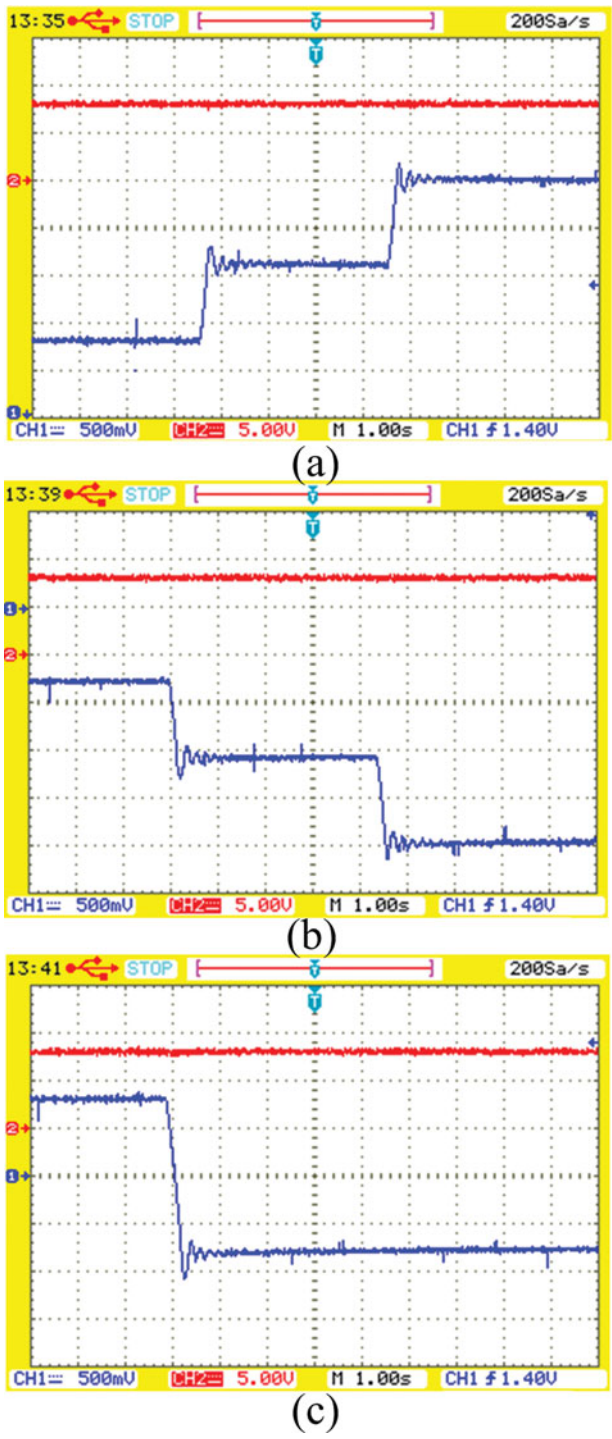

FIGURE 6. Experimental response of two-level DTC: (a) Forward motoring (speed increase). (b) Forward motoring (speed decrease). (c) Variation of speed from reverse motoring to forward motoring. (Red: Flux and 1 Div = 0.5 Wb) (Blue: Actual speed and 1 Div = 50 rad/sec).

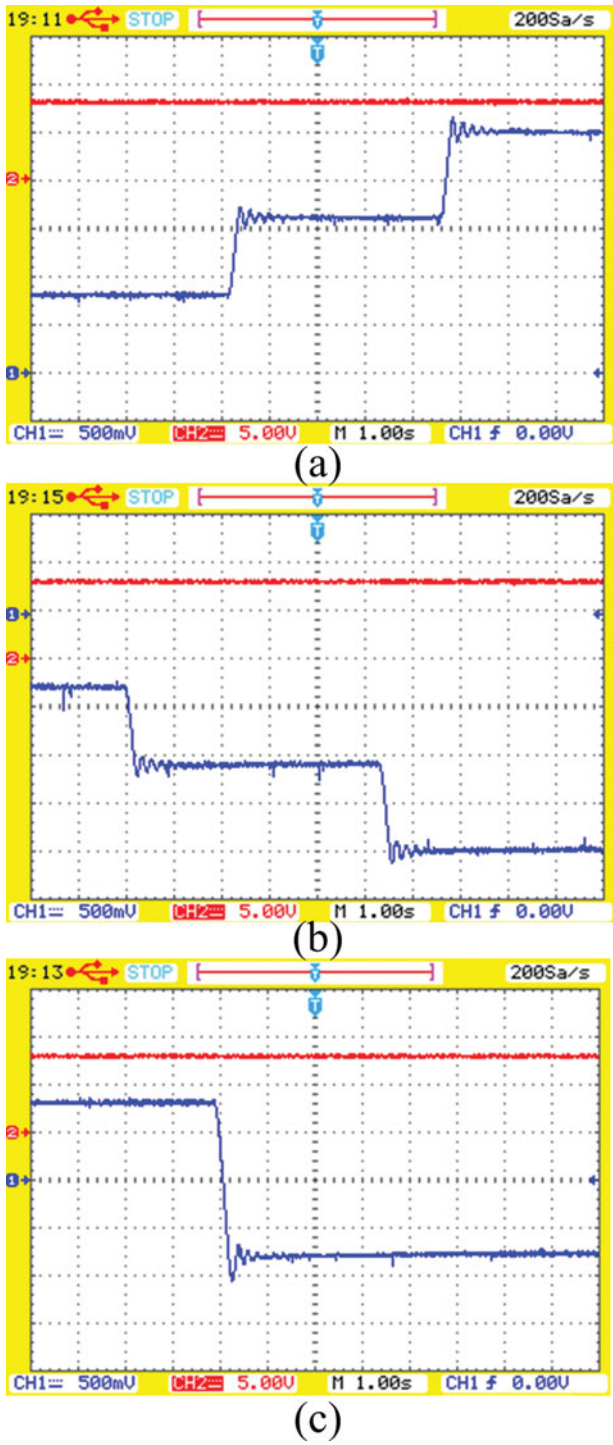

FIGURE 7. Experimental response of proposed DTC: (a) Actual speed and flux in forward motoring. (b) Actual speed and flux in reverse motoring. (c) Actual speed and flux during speed reversal. (Red: Flux and 1 Div = 0.5 Wb) (Blue: Actual speed and 1 Div = 50 rad/sec).

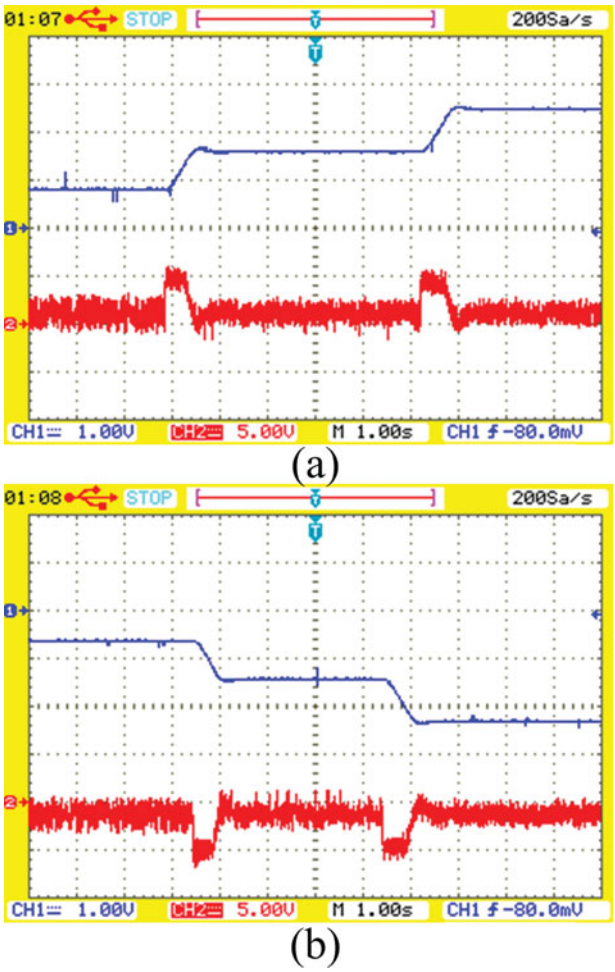

FIGURE 8. Experimental response of two-level DTC: (a) Actual speed and torque in forward motoring. (b) Actual speed and torque in reverse motoring (Red: Torque and 1 Div = 5 N-m) (Blue: Speed and 1 Div = 100 rad/sec).

reverse motoring and motor drive is set to operate at 0.8 Wb with variation of speeds −80 rad/sec, −160 rad/sec, and −250 rad/sec for two-level and proposed DTC.

Figures 6(c) and 7(c) indicate actual speed and flux of motor drive in forward and reverse motoring with variations of speeds 80 rad/sec and −80 rad/sec for two-level and proposed DTC. From experimental results, proposed four-level DTC gives less flux ripple in forward and reverse motoring conditions and the dynamic response of proposed DTC is better. Figures 8(a) and 9(a) indicate actual speed and electromagnetic torque of motor drive in forward motoring with speed variations of 80 rad/sec, 160 rad/sec, and 250 rad/sec for two-level and proposed DTC. Figures 8(b) and 9(b) indicate actual speed and torque of motor drive in reverse motoring with variations of speed −80 rad/sec, 160 rad/sec, and 250 rad/sec for two-level DTC and proposed DTC. From Figures 8 and 9, proposed four-level DTC gives less torque ripple in steady-state during forward and reverse motoring modes when compared with two-level DTC.

Figure 10 indicates A-phase voltage, common mode voltage of two-level and proposed DTC. Figure 11 is to compare steady-state torque ripple of conventional and proposed DTC at different frequencies of operation. The tabulated numerical data of torque ripple are obtained under steady-state conditions.

From Figures 5–10, it is observed that at high speed (250 rad/sec), medium speed (160 rad/sec), and low speed (80 rad/sec), the proposed four-level DTC gives less flux and torque ripples during forward motoring and reverse motoring when compared with two-level DTC of open end winding induction motor.

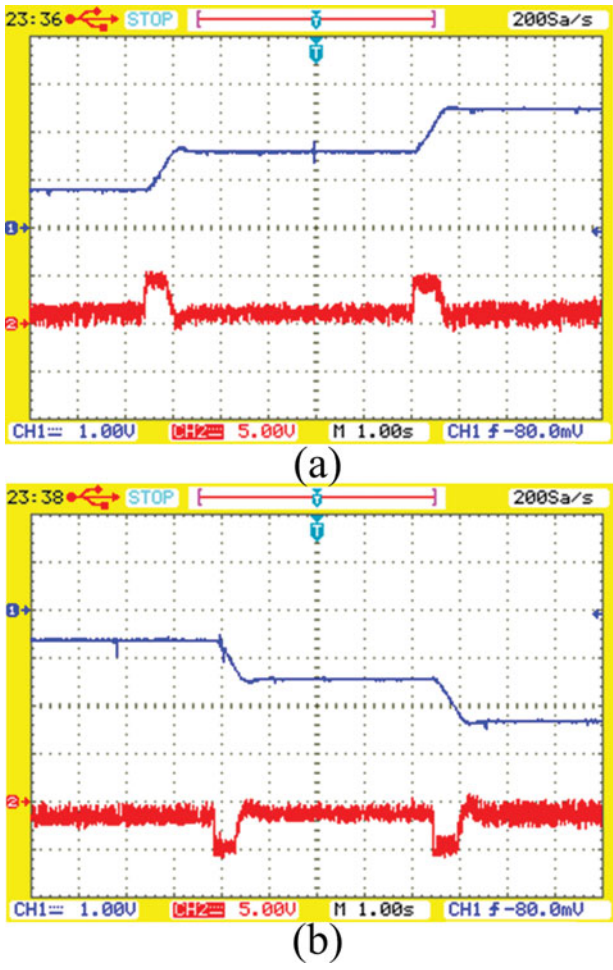

FIGURE 9. Experimental response of proposed DTC: (a) Actual speed and torque in forward motoring. (b) Actual speed and torque in reverse motoring (Red: Torque and 1 Div = 5 N-m) (Blue: Speed and 1 Div = 100 rad/sec).

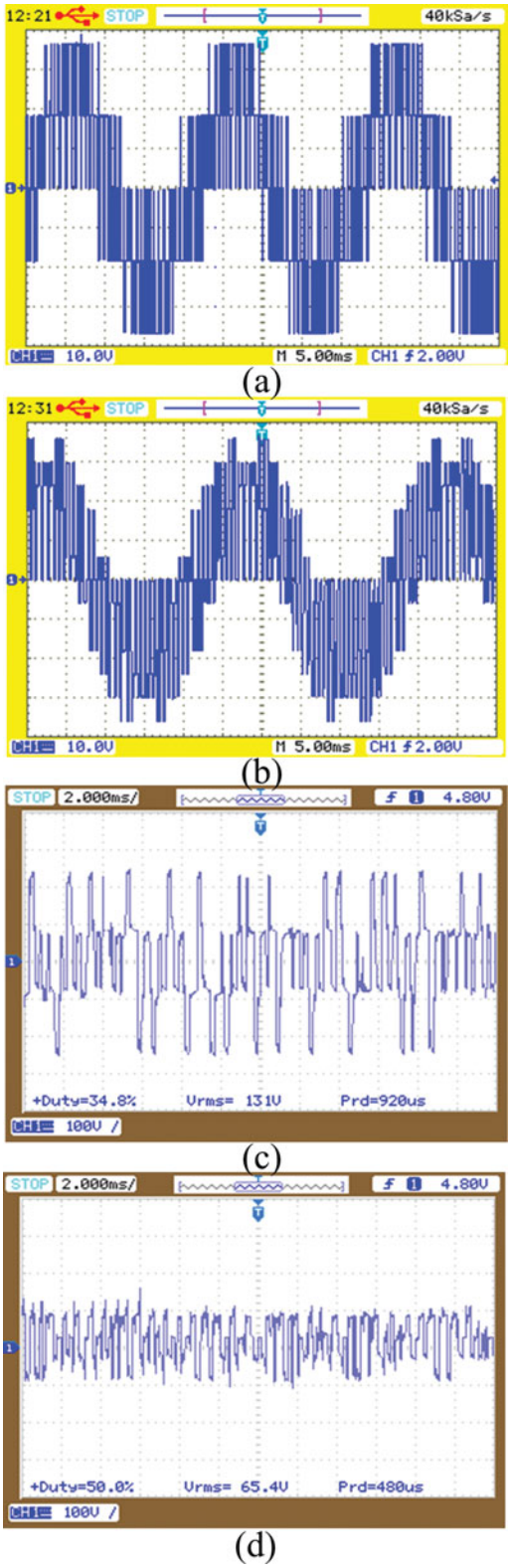

FIGURE 10. Experimental response of a-phase voltage at a speed of 250 rad/sec: (a) Two-level DTC. (b) Proposed DTC. (c) Common mode voltage in two-level DTC, and (d) Common mode voltage in proposed DTC (1 Div = 100 V).

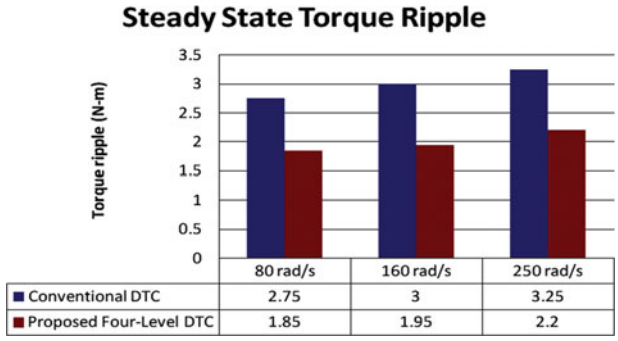

	80 rad/s	160 rad/s	250 rad/s
Conventional DTC	2.75	3	3.25
Proposed Four-Level DTC	1.85	1.95	2.2

FIGURE 11. Summary of experimental results for steady-state torque ripple.

4. CONCLUSION

In this paper, an effective voltage switching state algorithm implemented to four-level voltage configuration by using two two-level inverters for direct torque controlled open end winding induction to reduce torque and flux ripple at different operating speed conditions. In this paper, the motor drive is tested at various speeds and the motor drive is operated in forward and reverse motoring conditions with speeds of 80 rad/sec, 160 rad/sec, and 250 rad/sec. The proposed DTC can be used in electric vehicles, industries, marines, ship propulsion and it can be used for high dynamic performance applications. The limitation of the proposed DTC is that for field weakening operation, the proposed DTC is not preferable. From the experimental results, for all operating speeds the proposed DTC scheme reduces flux and torque ripples when compared with conventional two-level DTC. Implementation of proposed DTC is simple and it provides all features of conventional DTC. The proposed DTC can also applicable for PMSM. Application of model predictive control for the proposed DTC is left for future studies. The experiment has been carried using two voltage sensors, two current sensors, and speed encoder, the reduction of these sensors has left for future research work.

ORCID

Kunisetti V Praveen Kumar http://orcid.org/0000-0001-7384-961X
Thippiripati Vinay Kumar http://orcid.org/0000-0002-7250-6655

REFERENCES

[1] Kumar, A., Fernandes, B. G., and Chatterjee, K., "Direct torque control of open-end winding induction motor drive using the concept of imaginary switching times for marine propulsion systems," IEEE-PESC-04, Vol. 2, pp. 1214–1219, Nov. 2005.

[2] Takahashi, I., and Noguchi, T. "A new quick-response and high-efficiency control strategy of an induction motor," *IEEE Trans. Ind. Appl.*, Vol. 22, No. 5, pp. 820–827, 1986. doi:10.1109/TIA.1986.4504799.

[3] Baader, U., Depenbrock, M., and Gierse, G., "Direct self control (DSC) of inverter-fed-induction machine – A basis for speed control without speed measurement," *IEEE Trans. Ind. Appl.*, Vol. 28, pp. 581–588, 1992. doi:10.1109/28.137442.

[4] Casadei, D., Profumo, F., Serra, , and Tani, A. "FOC and DTC: Two viable schemes for induction motors torque control," *IEEE Trans. Power Electron.*, Vol. 17, No. 5, pp. 779–787, 2002. doi:10.1109/TPEL.2002.802183.

[5] Idris, N. R. N., and Yatim, A. H. M. "Direct torque control of induction machines with constant switching frequency and reduced torque ripple," *IEEE Trans. Ind. Elec.*, Vol. 51, No. 4, 758–767, August 2004. doi:10.1109/TIE.2004.831718.

[6] Sutikno, T., Idris, N. R. N., and Jidin, A. "A review of direct torque control of induction motors for sustainable reliability and energy efficient drives," *Renew. Sustain. Energy Rev.*, Vol. 32, pp. 548–558, 2014. doi:10.1016/j.rser.2014.01.040.

[7] Kang, J. K., and Sul, S. K. "New direct torque control of induction motor for minimum torque ripple and constant switching frequency," *IEEE Trans. Ind. Appl.*, Vol. 35, No. 5, pp. 1076–1082, 1999. doi:10.1109/28.793368.

[8] Zhang, J., and Rahman, M. F. "Analysis and design of a novel direct flux control scheme for induction machine," Proc. Int. Conf. on IEMDC, pp. 426–430, San Antonio, TX, 2005.

[9] Kumar, T. V., and Rao, S. S. "Modified direct torque control of three phase induction motor drives with low ripple in flux and torque," *Leonardo J. Sci. (LJS).*, Vol. 10, No. 18, pp. 27–44, 2011.

[10] Noguchi, T., Yamamoto, M., Kondo, S., and Takahashi, I. "Enlarging switching frequency in direct torque-controlled inverter by means of dithering," *IEEE Trans. Ind. Appl.*, Vol. 35, No. 6, pp. 1358–1366, 1999. doi:10.1109/28.806050.

[11] Ambrožic, V., Buja, G. S., and Menis, R. "Band-constrained technique for direct torque control of induction motor," *IEEE Trans. Ind. Appl.*, Vol. 51, No. 4, pp. 776–784, 2004.

[12] Vinay Kumar, T., and Rao, S. S. "Hardware Implementation of direct load angle controlled induction motor drive," *Electric Power Comp. Syst.*, Vol. 42, No. 14, pp. 1532–5008, 2014.

[13] Kumar, T. V., and Rao, S. S. "Direct load angle of three phase induction motor drives," IEEE PEDS 2011, pp. 513–516, Singapore, 5–8 December 2011.

[14] Kumar, T. V., and Rao, S. S. "Direct torque controlled induction motor drive based on cascaded three two-level inverters," *Int. J. Model. Simul.*, Vol. 34, No. 2, pp. 70–82, 2014. doi:10.2316/Journal.205.2014.2.205-5849.

[15] Babaei, M., and Heydari, H. "Direct torque control of pulse width modulation current source –inverter fed induction motor by novel switching method," *Electric Power Comp. Syst.*, Vol. 38, pp. 514–532, 2010. doi:10.1080/15325000903376933.

[16] Salem, F. B., and Derbel, N. "Direct torque control of induction motors based on discrete space vector modulation using adaptive sliding mode control," *Electric Power Comp. Syst.*, Vol. 42, pp. 1598–1610, 2014. doi:10.1080/15325008.2014.927029.

[17] Scotock, J., Geyer, T., and Madawala, U. K. "A comparison of model predictive control schemes for MV induction motor drives," *IEEE Trans. Ind. Inf.*, Vol. 9, No. 2, pp. 909–919, May 2013. doi:10.1109/TII.2012.2223706.

[18] Smoasekhar, V. T., Gopa kumar, K., Baiju, M. R., and Mohapatra, K. K. "A multi level inverter system for an induction motor with open end windings," *IEEE Trans. Ind. Elec.*, Vol. 52, No. 3, pp. 824–836, JUNE 2005. doi:10.1109/TIE.2005.847584.

[19] Rahim, M. K., Patkar, F., Jidin, A., Ahmadi, M. Z. R. Z., Firdaus, R. N., Halim, W. A., and Razi, A. " Reduced torque ripple and switching frequency using optimal DTC switching strategy for an open-end winding of induction machines," *IEEE PEDS* 2015, Sydney, Australia, pp. 767–772, 9–12 June 2015.

[20] Kalaiselvi, J., and Srinivas, S. "Bearing currents and shaft voltage reduction in dual inverter fed open end winding induction motor with reduced CMV PWM methods," *IEEE Trans. Ind. Ele.*, Vol. 62, pp. 144–152, 2015. doi:10.1109/TIE.2014.2336614.

[21] Reddy, B. V., and Somasekhar, V. T. "A dual inverter fed four-level open end winding induction motor with a nested rectifier-inverter," *IEEE Trans. Ind. Ele.*, Vol. 9, pp. 938–946, 2013.

[22] Vas, P. "*Sensorless Vector and Direct Torque Control*," Oxford University Press, USA, 1998.

[23] Nabae, A., Ogasawara, S., and Akagia, H. "Novel control scheme for current controlled PWM inverters," *IEEE Trans. Ind. Appl.*, Vol. IA-22, No. 4, pp. 696–701, 1986. doi:10.1109/TIA.1986.4504780.

APPENDIX

Experimental Set-Up

The experimental set-up is used to verify, proposed four-level DTC scheme of open end winding induction motor developed by using d-Space 1104 control board. The photograph of experimental set-up is shown in Figure A.1. This photo consists of a 4-pole, 5-H.P, 50-Hz, 3-phase, 415 V, 7.54 A, 1440 RPM induction motor with open end windings. Induction motor is fed with two two-level voltage source inverters operating Dual-mode. The inverters are driven by controlling pulses generated from d-space 1104. The d-space DS1104 R&D board is used as an interface between MATLAB RTI model and motor drive.

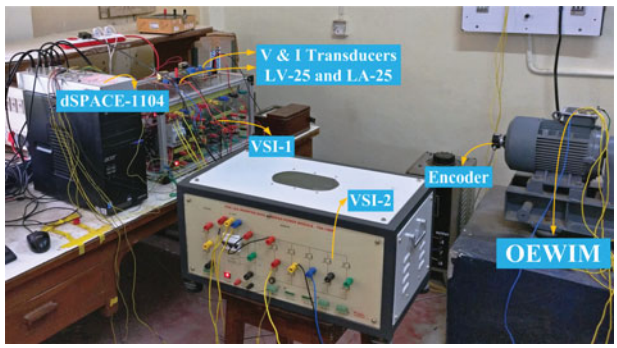

FIGURE A.1. Photograph of experimental setup.

BIOGRAPHIES

Kunisetti V Praveen Kumar received his B.Tech degree in electrical and electronics engineering and his M.Tech degree from JNTU, Kakinada, India in the years 2011 and 2015, respectively. He is currently working toward his Ph.D. degree in the Department of electrical engineering, National Institute of Technology, Warangal, India. His research interests are direct torque control, predictive torque control, multi-level inverters, and open-end induction motor drives.

Thippiripati Vinay Kumar received his B.Tech degree in electrical and electronics engineering from JNTU, Hyderabad, India, in 2005 and M.Tech, degree from JNTU, Hyderabad, India, in 2008. He received his Ph.D. degree from National Institute of Technology, Warangal, India, in 2015. Since 2013, he is working as an Assistant professor in National Institute of Technology, Warangal, India. His research interests are power electronics and drives, direct torque control, predictive torque control, open-end winding induction motor drives, multi-level inverters, hybrid electric vehicles and renewable energy.